 doi:10.20944/preprints202102.0501.v1

Article

Age-dependent Non-Silent Somatic Mutation with Transcriptomic Landscape and Prognosis of Lower Grade Glioma

YoungJoon Park[1,2,#], JeongMan Park[1,2,#], Ju Won Ahn[1,2], JeongMin Sim[2], Su Jung Kang[1,2], Suwan Kim[2], Sojung Hwang[2,3], Kyoung Su Sung[4,*,‡] and Jaejoon Lim[2,*,‡]

[1] Institute Department of Biomedical Science, College of Life Science, CHA University, Seongnam, Gyeonggi-do 13488, Korea
[2] Department of Neurosurgery, Bundang CHA Medical Center, CHA University College of Medicine, Seongnam, Gyeonggi-do 13496, Korea
[3] Global Research Supporting Center, Bundang CHA Medical Center, CHA University College of Medicine, Seongnam, Gyeonggi-do 13496, Korea
[4] Department of Neurosurgery, Dong-A University Hospital, Dong-A University College of Medicine, Busan 49201, Korea
* Correspondence: coolppeng@naver.com; Tel.: +82-31-780-5688(JJ Lim.); sungks1465@gmail.com; Tel.: +82-51-240-5241(KS Sung)
# These authors contributed equally as Co-first authors.
‡ These authors contributed equally as Co-last authors.

Abstract: Glioma accounts for 80% of all malignant brain tumors and is the most common adult primary brain tumor. Age is an important factor affecting the development of cancer as somatic mutations accumulate with age. In this study, we aimed to analyze the significance of age-related non-silent somatic mutations in glioma prognosis. Histological tumor grade depends on age at diagnosis in patients with *IDH1*, *TP53*, *ATRX*, and *EGFR* mutations. The hierarchical clustering of patients was dominantly separated by *IDH1* and *EGFR* mutations. Furthermore, patients with *IDH1* mutation were dominantly separated by *TP53* and *ATRX* double mutation and its double wildtype counterpart. Patients with the double mutation showed poorer prognosis than those with the double wild type genotype. In conclusion, among the many somatic mutations, those in *IDH1*, *TP53*, *ATRX*, and *EGFR* are important for glioma classification based on histological grade and related with onset age. Patients with *EGFR* mutation which showed late onset had the poorest prognosis, whereas those with only *IDH1* mutation showed early onset had the best prognosis.

Keywords: age; glioma; mutation; TCGA; transcriptomic analysis

1. Introduction

Glioma, accountings for 80% of all malignant brain tumors, is the most common primary brain tumor in adults [1], and is usually treated using radiation therapy and using Temozolomide treatment after maximal safe resection [2]. Histologically, gliomas are classified as lower grade glioma (LGG) [World Health Organization (WHO) grade 2 (G2) and 3 (G3)] and glioblastoma multiforme (GBM) [WHO grade 4 (G4)]. LGG has a better prognosis than GBM, and the sensitivity of treatment depends on the molecular subtype of LGG in perspective of overall survival (OS) and progression free survival (PFI). In contrast, GBM has poor prognosis, and the development of new treatment methods based on its molecular characteristics is difficult because of infiltrative and integrative characteristics to normal brain tissues [3, 4].

Age is an important factor affecting the development of cancer. Most adult cancers develop exponentially with age [5], owing to the accumulation of somatic mutations [5-7]. However, all accumulated mutations do not contribute to cancer development. A mutation that contributes to the development of cancer is called a driver; a driver undergoes positive selection in the tissue microenvironment and leads to the development of cancer cell characteristics, such as cell growth [7, 8].

Preprints (www.preprints.org) | NOT PEER-REVIEWED | Posted: 23 February 2021 doi:10.20944/preprints202102.0501.v1

Current studies suggest signature mutation of glioma, but age-related mutation and related transcriptomic patterns are not reported yet. In this study, we investigated the effects of age to occurrence of non-silent somatic mutations on glioma prognosis and analyzed their transcriptomic significance using The Cancer Genome Atlas (TCGA) transcriptomic data. Finally, results of this study can be applied to molecular theraphy with age and prediction of prognosis.

2. Results

2.1. Identification of Age-related Non-silent Mutations in LGG and GBM

Clinical data and non-silent somatic mutation data by multi-center mutation calling (MC3) from TCGA were used to identify somatic mutations associated with age. Using logistic regression analysis, we analyzed whether age at diagnosis affects somatic mutations in LGG (Table S1) and GBM (Table S2). Results showed that, in patients with LGG, *IDH1*, *ATRX*, and *TP53* were less likely to mutate with aging, while *EGFR* acquired more mutations with aging (p-value < 0.05 after Bonferroni correction) (Figure 1a). Similar to LGG, *ATRX* was less likely to mutate with age in GBM (p-value < 0.05 after Bonferroni correction) (Figure 1b). Additional mutations information of four genes was included supplementary table S3.

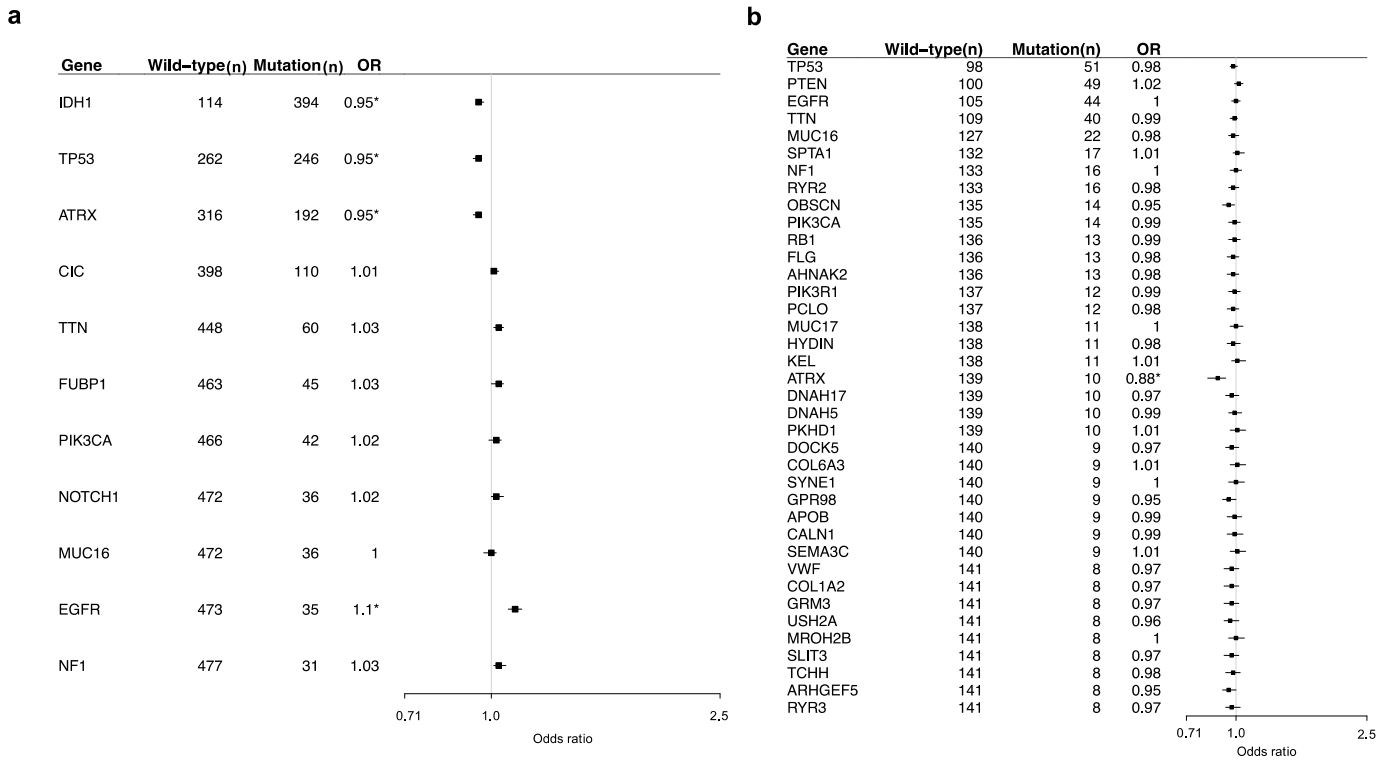

Figure 1. Frequencies of mutated and wild-type genes and logistic regression results showing the relationship of mutations with age in patients with lower grade glioma (a) and glioblastoma (b). Genes shown have mutation rates > 5%. OR, odds ratio; *, significant.

2.2. Histological Tumor Grade Depends on Age at Diagnosis in the IDH1 Wild-type group but not in the Mutant group

The patterns of age and *IDH1* mutations were analyzed according to histological tumor grade. Results showed that, in patients with *IDH1* wild-type, as the histologic tumor grade increased, the onset age of glioma was increased (Figure 2a). However, in *IDH1*

Preprints (www.preprints.org) | NOT PEER-REVIEWED | Posted: 23 February 2021 doi:10.20944/preprints202102.0501.v1

mutant patients, despite the rising histologic tumor grade of cancer, the onset age of glioma was constant (Figure 2a). In patients with G2 and G3 tumors, overall survival (OS) differed significantly between patients with and without *IDH1* mutation (log-rank *p*-value in G2: 0.002; in G3: 1E-11; in G4; 0.02) (Figure 2b and table S4). In particular, the OS of patients with *IDH1* wild-type and LGG did not differ significantly from that of patients with *IDH1* mutation in GBM patients, but median survival was lower (median survival; *IDH1* wild-type in LGG: 758 and *IDH1* mutant in GBM: 1,024) (Figure 2b).

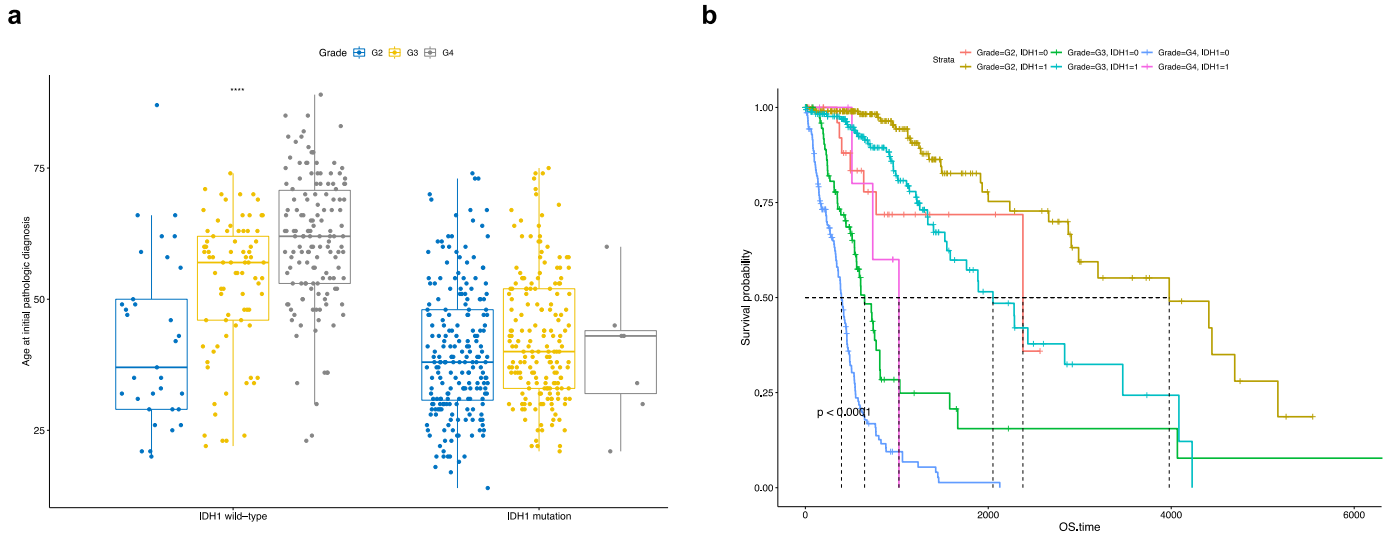

Figure 2. Comparison of tumor grades of patients with *IDH1* wild-type and *IDH1* mutation with respect to age at initial pathologic diagnosis. p-value < 0.001 and 0.0001 are indicated by *** and ****, respectively. ns, not significant (a). Survival analysis comparing patients with *IDH1* wild-type or *IDH1* mutation in each tumor grade. Time up to which 50% patients survived is shown by the dotted line in every types (b).

2.3. Transcriptomic Landscape of Tumors of Different Histological Grades Harboring IDH1 Mutations

To determine the transcriptomic landscape of tumors of different histological grades harboring *IDH1* mutation, we performed a multi-label information gain (IG)-based feature selection of genes that possess discriminatory power according to combinations of histological tumor grades and *IDH1* mutation statuses (Table S5). As a result, a hierarchical tree of patients dominantly separated by LGG and GBM was generated (Figure 3a). Interestingly, the gene expression pattern of *IDH1* wild-type of G3 was similar to *IDH1* wild-type of G4. In the IDH1 wild-type of G4 and G3-riched cluster, genes involved in the mitotic cell cycle and degradation of the extracellular matrix which are associated with malignancy of tumor in the Reactome 2020 database were more highly expressed than in LGG (Figure 3).

Preprints (www.preprints.org) | NOT PEER-REVIEWED | Posted: 23 February 2021 doi:10.20944/preprints202102.0501.v1

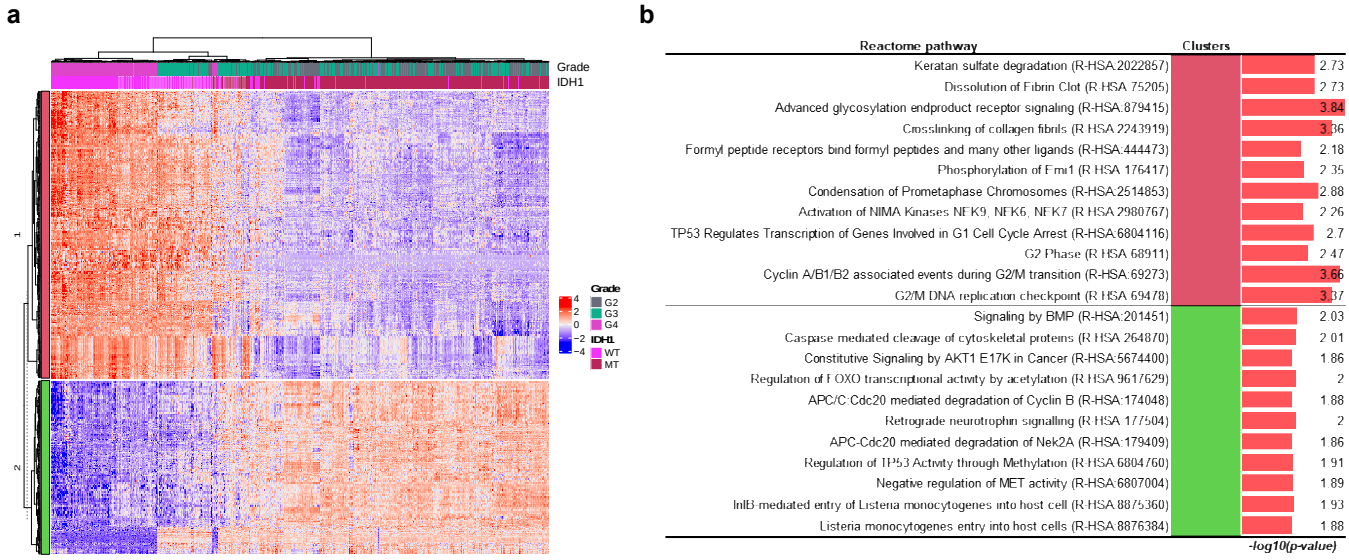

Figure 3. Heatmap with hierarchical tree of patients by gene expression pattern with information gain (IG) over 0.35. The top annotations show tumor grade and mutation status (*IDH1* mutant or wild-type). WT indicates wild-type; MT indicates mutation (a). Statistically significant results of the pathway enrichment analysis of gene clusters in the *IDH1* hierarchical group (b).

2.4. Distribution and Prognosis of Age-related Non-silent Somatic Mutations in LGG

Among several somatic mutations of four genes associated with pathological onset age in LGG, mutation pattern analysis revealed that *ATRX* and *TP53* mutations occurred predominantly in patients with *IDH1* mutations. The *EGFR* mutations dominantly occurred in patients with *IDH1* wild-type (Figure 4a). The proportion of patients who divided by mutation status are suggested in supplementary (Table S6). The group with *EGFR* mutations had the worst prognosis, in terms of both OS and progression-free interval (PFI) (Figure 4b and Table S7). Among patients with *IDH1* mutations, those with *ATRX* and *TP53* mutations showed poorer PFI than those with the wild-type genes (Figure 4b).

Preprints (www.preprints.org) | NOT PEER-REVIEWED | Posted: 23 February 2021 doi:10.20944/preprints202102.0501.v1

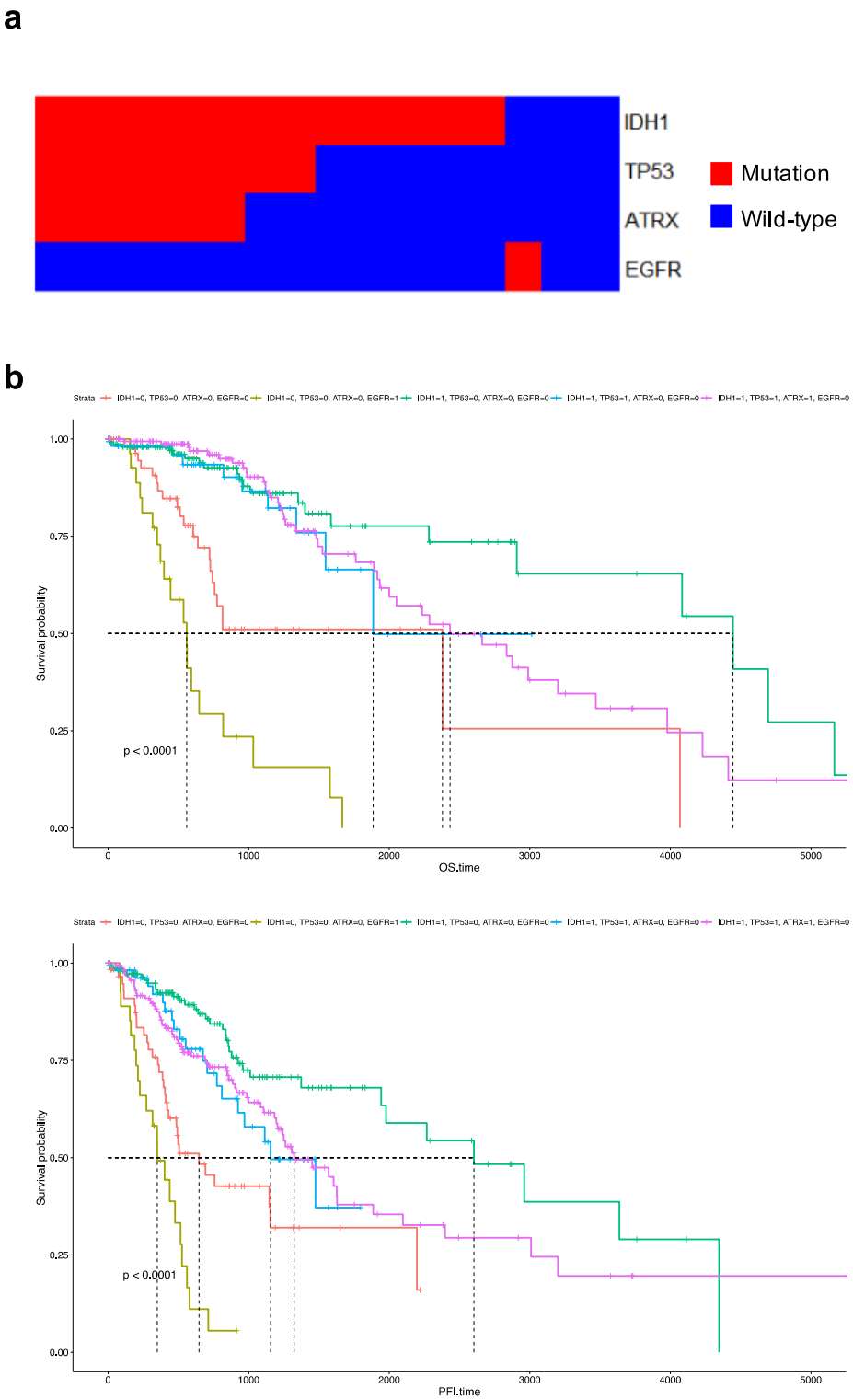

Figure 4. Mutational patterns of *IDH1*, *TP53*, *ATRX*, and *EGFR* in the hierarchical tree (a). Survival analysis of patients with mutant or wild-type genes in terms of overall survival and progression-free survival (b). 0 indicates wild-type; 1 indicates mutation.

2.5. ATRX and TP53 Mutation Occurred in Patients with Early Onset Age of G2 and G3 Glioma and IDH1 Mutation, and the Gene Expression Patterns of Mutant ATRX and TP53 in LGG Differed from those of their Wild-type counterpart

ATRX and *TP53* mutations were common in patients with *IDH1* mutation and were associated with the age of onset of LGG (Figure 4a). Therefore, we analyzed whether

Preprints (www.preprints.org) | NOT PEER-REVIEWED | Posted: 23 February 2021 doi:10.20944/preprints202102.0501.v1

ATRX and *TP53* mutations were directly related to the early age of onset of patients with *IDH1* mutation. Results showed that both *ATRX* and *TP53* mutations occurred in patients with early onset age of G2 and G3 tumors (Figure 5a). In the transcriptomic analysis, the hierarchical tree of patients primarily clustered by *ATRX* and *TP53* double mutations and their double wild-type versions rather than by histological grade (Figure 5b). In total, 121 genes passed the IG-based feature selection. Among these 121 genes, the telomere extension-related Reactome term was significantly enriched in the gene enrichment test. This term contained only *TERT* (Figure 5c, Table S8).

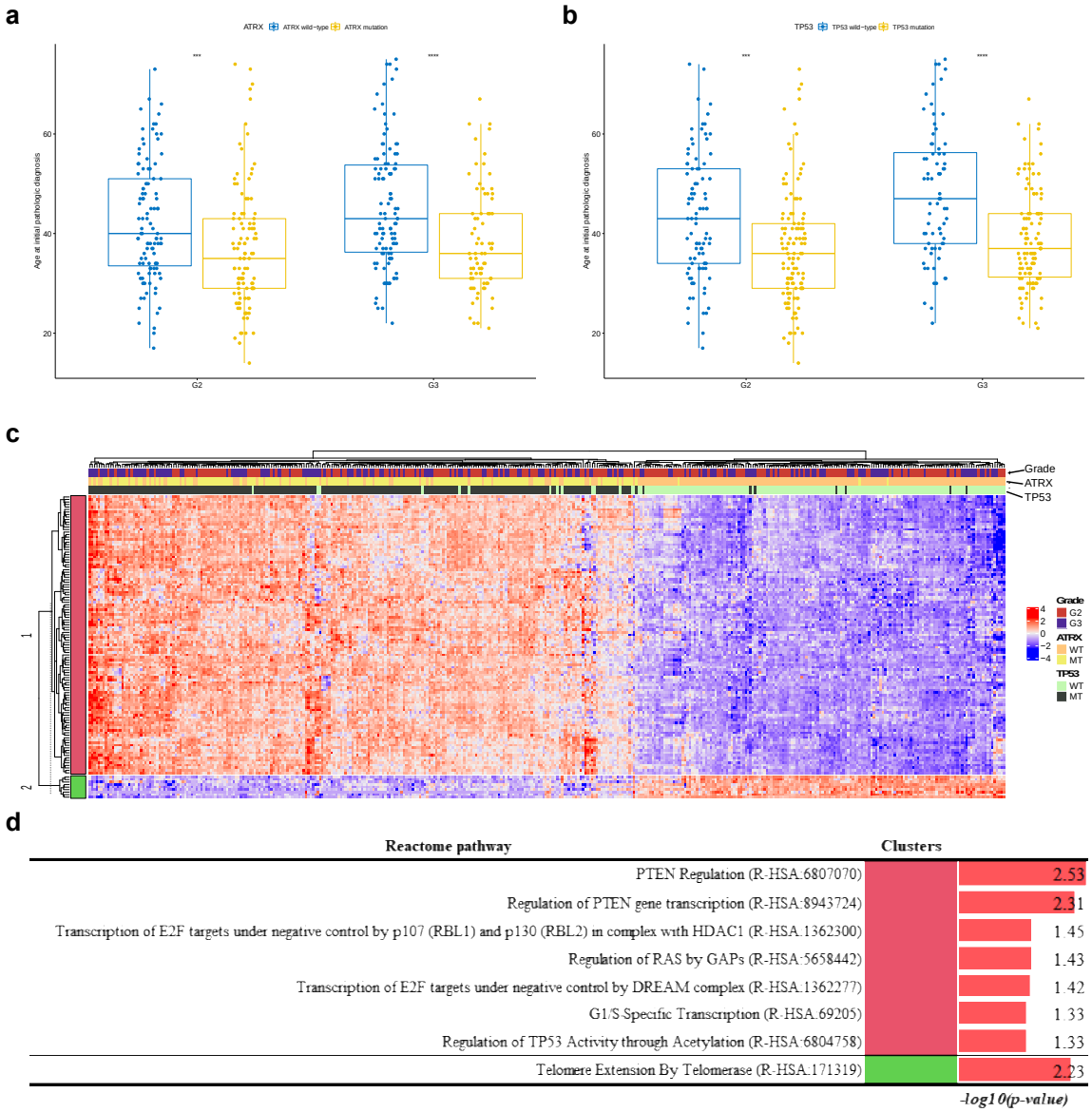

Figure 5. Comparison of patients harboring *ATRX* and *TP53* wild-type and mutation with age of glioma onset at initial pathological diagnosis in the background of *IDH1* mutation. p-values less than 0.001 and 0.0001 are shown by *** and ****, respectively. As the number of GBM patients with *IDH1* mutation is few, GBM is excepted in analysis (a). Heatmap with the hierarchical tree of patients by gene expression pattern with information gain (IG) over 0.35. The top annotations show the grade and mutational status (mutant or wild-type) of *ATRX* and *TP53*. WT indicates wild-type; MT indicates mutation (b). Statistically significant results of pathway enrichment analysis of gene clusters in the *ATRX* and *TP53* hierarchical group (c).

2.6. TERT Expression was Suppressed in LGG and GBM with ATRX Non-silent Mutations

Preprints (www.preprints.org) | NOT PEER-REVIEWED | Posted: 23 February 2021 doi:10.20944/preprints202102.0501.v1

We observed that *TERT* expression which is only significant in cluster 2 was related to *ATRX* and *TP53* double mutation in the *IDH1* wild-type subgroup in LGG (Figure 5b). In addition, *TERT* expression was highly suppressed in *ATRX* and *TP53* double mutant patients in the *IDH1* mutation subgroup in LGG (Figure 6a). Figure 4a shows that the *ATRX* and *TP53* mutation patterns were similar. Therefore, we compared *TERT* expression with the *ATRX* or *TP53* mutation status and tumor grade. *TERT* expression was highly suppressed in patients with *ATRX* mutation for all histological tumor grades, but not in those with *TP53* mutation of G4 (Figure 6b). It indicated that the *TERT* expression was tightly regulated by *ATRX* but not *TP53* mutation.

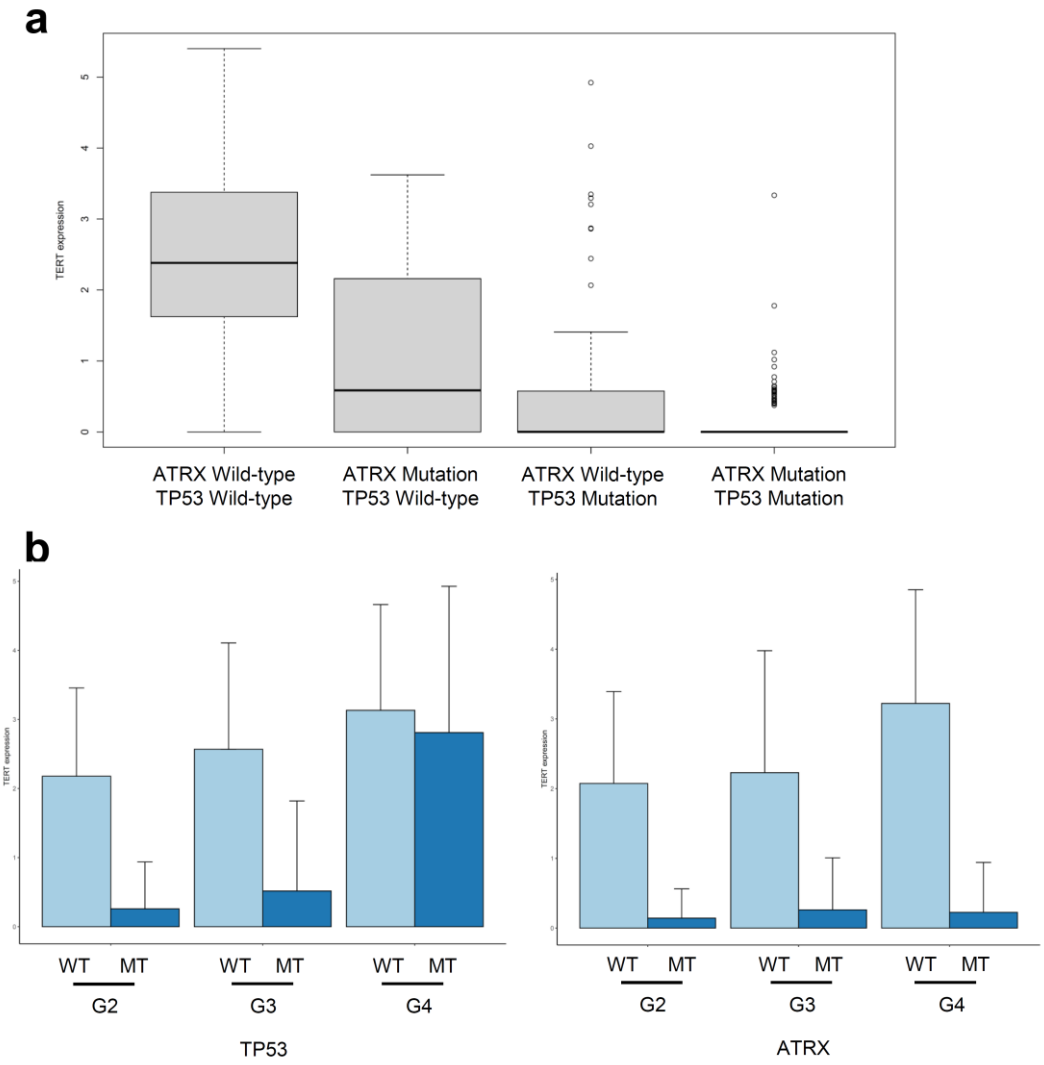

Figure 6. Variation in *TERT* expression level with the mutation statuses of *ATRX* and *TP53* in tumors with *IDH1* mutation (a). *TERT* expression level in tumors with *IDH1* mutation with separated mutation statuses of *ATRX* and *TP53* for each grade. WT indicates wild-type; MT indicates mutation (b).

2.7. EGFR Mutation Occurred at Late Onset Age in Patients with G3 tumor and was Associated with Poor Prognosis of GBM Patients but not was not Clustered in Transcriptomic Analysis

Unlike *ATRX*, *TP53*, and *IDH1* mutations, *EGFR* mutations were more frequent in older patients. Age at initial pathologic diagnosis of patients with *EGFR* wild-type showed positive correlation with tumor grade. Interestingly, in G2 and G3 patients who have relatively an early onset age, the patients with EGFR mutation were occurred tumor at old age as well as G4. In addition, despite having LGG, patients with *EGFR* mutations in G3

Preprints (www.preprints.org) | NOT PEER-REVIEWED | Posted: 23 February 2021 doi:10.20944/preprints202102.0501.v1

showed poor prognosis similar to those of GBM patients (Figure 7b). In the transcriptomic analysis, the hierarchical tree of patients was dominantly divided into G2 and the rest, but not by *EGFR* mutation status (Figure 7c, Table S9). Most of the significant pathways in the pathway enrichment analysis were related to the regulation of the cell cycle and were downregulated in GBM (Figure 7d).

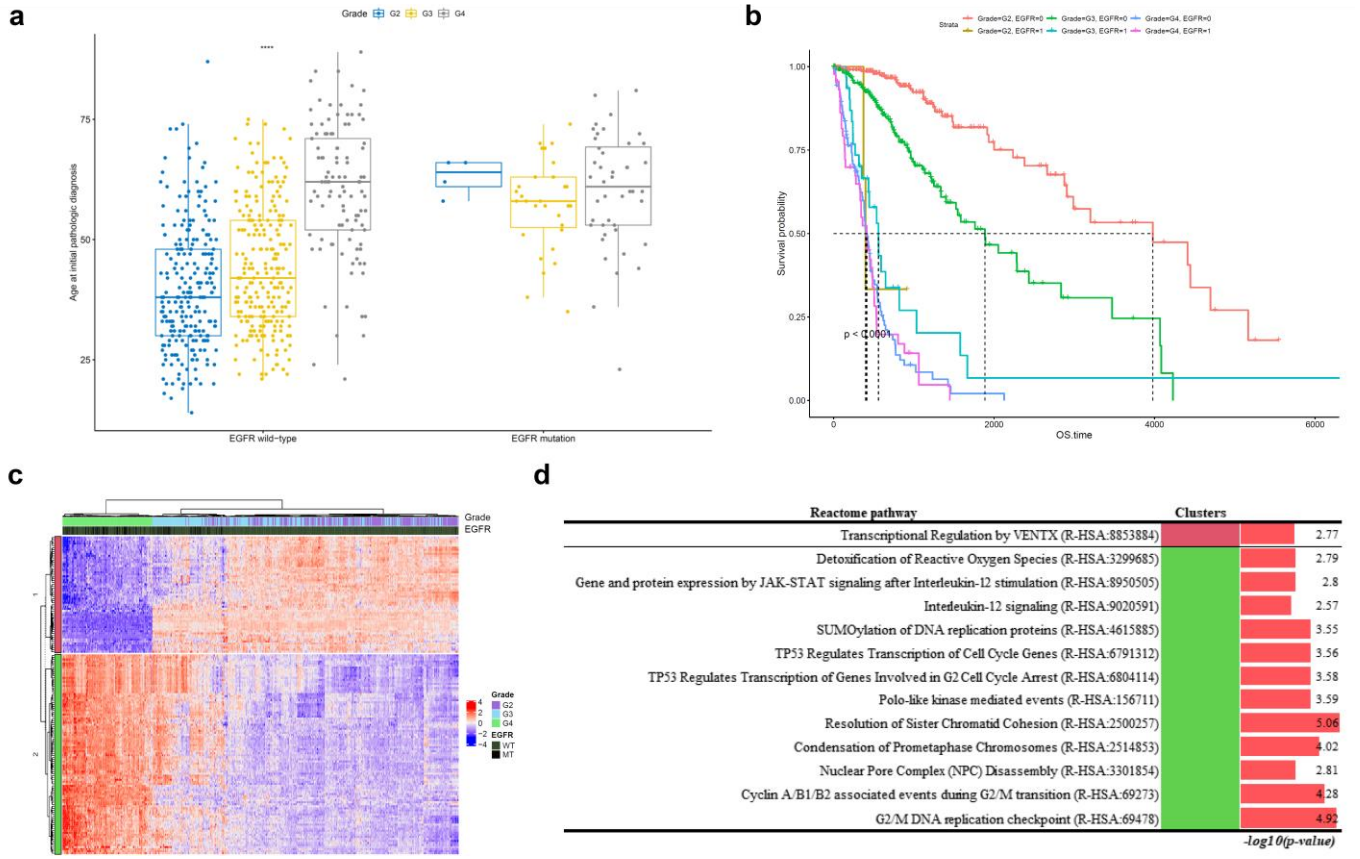

Figure 7. Comparison of ages at initial pathological diagnosis of tumors with *EGFR* wild-type and those with *EGFR*. p-values less than 0.01 and 0.0001 are shown as ** and **** respectively. ns, not significant (a). Survival analysis comparing *EGFR* mutant or wild-type and each grade with overall survival. 0 indicates wild-type; 1 indicates mutation (b). Heatmap with hierarchical tree of patients based on gene expression pattern with IG over 0.35. Top annotations show tumor grade and genotype (mutant or wild-type) of *EGFR*. WT indicates wild-type; MT indicates mutation (c). Statistically significant results of pathway enrichment analysis of gene clusters in the *EGFR* hierarchical group (d). Mutational pattern of GBM (e). Comparison of *EGFR* expression levels between tumors with *EGFR* mutant and those with *EGFR* wild-type against an *IDH1* wild-type background (f).

3. Discussion

Cancer is highly related with the occurrence of somatic mutations, which accumulate with age [9, 10]. In this study, we deeply investigated characteristics of molecular features and expression patterns of age-related somatic mutations in glioma.

IDH1 mutation is an important classifying point in both LGG and GBM [11]. In *IDH1* mutant, conversion of α-ketoglutarate to 2-hydroxyglutarate (2-HG) is reduced, and increases the 2-HG level in patients by 100 folds [12]. Accumulation of 2-HG suppresses cell growth and also induces ferroptosis [13]. In the *IDH1* mutation group, cell-cycle-related genes are down-regulated in contrast to *IDH1* wild-type group (Figure 3a, b). However, hypermethylation of *TP53* occurs in *IDH1* mutant, owing to the accumulation of 2-HG [14]. In contrast, regulation of *TP53* expression via methylation does not occur against the *IDH1* wild-type background. Hypermethylation of DNA in *IDH1* mutants results in the

 doi:10.20944/preprints202102.0501.v1

formation of the oncometabolite, 2-HG [15]. In short, most patients of grade 2 and 3 tumors with *IDH1* mutation show suppression of cell growth and high methylation of *TP53*, resulting in the down-regulation of *TP53* transcription in younger glioma patients. In contrast, promotion of cell growth and low methylation of *TP53* are observed in most patients of grade 4 and a few of grade 3 tumors with *IDH1* wild-type in older patients. Cell migration reactome terms were also included in the analysis. In the *IDH1* wild-type background, degradation of keratan sulfate, which can interact with neuroregulatory ligands, dissolution of fibrin clot, and crosslinking of collagen fibrils, which are important for tumor cell and T cell migration, were higher than those in the *IDH1* mutant [16-18]. Activation of NIMA kinases, which induce premature mitosis, is highly activated in tumors with *IDH1* wild-type [19, 20]. Phosphorylation of early mitotic inhibitor (Emi1), which inhibits the anaphase-promoting complex/cyclosome (APC/C), is necessary for degradation of cyclins in mitosis [21]. APC/C with Cdc20 degrades type B cyclin and Nek2A and facilitates arrest of mitotic division [21-23]. Activity of Emi is lower for the *IDH1* wild-type background; in contrast, activation of APC/C is higher for the *IDH1* mutant background. In short, mitosis is suppressed more in tumors with *IDH1* mutation than in tumors with *IDH1* wild-type. Advanced glycosylation endproduct receptor signaling, which regulates cell proliferation, survival, differentiation, migration, and binding of formyl peptide receptors to formyl peptides and many other ligands, thereby regulating angiogenesis, cell proliferation and anti-apoptotic activities, is also higher in tumors with *IDH1* wild-type [24, 25]. In contrast, BMP signaling associated with glioma cancer stem cell signaling by AKT-E17K, which may enhance signaling for cell-cycle arrest and regulation of FOXO by acetylation, thereby increasing cell death and decreasing cell proliferation, is higher in *IDH1* mutant [26-28]. Negative regulation of mesenchymal epithelial transition and caspase-mediated cleavage of cytoskeleton, which are associated with morphological changes, are also higher in *IDH1* mutants [29, 30].

Unsupervised clustering revealed that mutations in *IDH1*, *TP53*, and *ATRX* occur simultaneously (Figure 4a). Onset of mutations in *TP53* and *ATRX* occur earlier in life, similar to onset of the *IDH1* mutation (Figure 5a, b). Mutation in *TP53*, a cell-cycle related oncogene, is prevalent in various types of cancer and occurs frequently in various glioma subtypes and glioblastoma [31, 32]. The main function of normal *TP53* involves the induction of cell-cycle arrest in the presence of DNA damage via binding to DNA and prevention of DNA replications [32]. Mutations in *ATRX*, which is mainly related to alternative lengthening of telomere (ALT) and regulation of epigenetic activity via methylation, are widely detected in glioma [33, 34]. Modulation of *TP53* by *ATRX* regulates the upstream events of cancer [35-37]. Using unsupervised clustering of gene set extracted via multi-label IG, patients were divided on the basis of *TP53* and *ATRX* double mutation and *TP53* and *ATRX* wild-type with *IDH1* mutation. (Figure 5b). PTEN regulation, negative control of transcription by E2F, and regulation of *TP53* via acetylation were upregulated in the double mutation group. However, telomere extension by telomerase was promoted in the double wild-type group. Interestingly, the level of TERT expression in patients with double mutation was almost zero (Figure 6a). After separating the mutations of *TP53* and *ATRX*, every patient with *ATRX* mutation showed a low level of TERT expression; however, TERT expression in patients with *TP53* mutation and a grade 4 tumor did not differ from that in the wild-type patients. TERT encodes telomerase reverse transcriptase, which preserves the length of telomeres [38]. Loss of function of TERT induces telomere shortening and cell senescene, a sign of permanent cell-cycle arrest [38]. In short, stabilization of telomeres by telomerase or ALT is associated with various primary cancer types and malignant tumors [39-41]. The results of this study showed the relationship between TERT expression and mutations in *ATRX* and *TP53*. Recent studies have reported that TERT expression prevents extension of telomeres by ALT, which increases loss of *ATRX*; conversely, decrease in TERT expression, which is linked to the hypomethylation of TERT promoter, precedes ALT in zebrafish [42, 43]. Another study reported that TERT expression is downregulated in cells with ALT [44]. In short, *ATRX* loss resulting from *ATRX* mutation induces an increase in ALT and reduces TERT expression in hypomethylation

Preprints (www.preprints.org) | NOT PEER-REVIEWED | Posted: 23 February 2021 doi:10.20944/preprints202102.0501.v1

of the TERT promoter, which is related to the positive control of TERT expression in human brain cancer [34, 45]. Regarding the relationship between *TP53* mutation and TERT expression, *TP53* is normally activated by DNA damage and induces p21 and cell-cycle arrest [46]. ATM-Chk2-p53 may also participate in the feedback regulation of TERT expression in lung cancer [46]. Conversely, the lack of *TP53* induces an increase in TERT expression [46]. *ATRX* and *TP53* mutations differentially affect TERT expression, although we can infer that the impact of *ATRX* mutation is more than that of the *TP53* mutation on prognosis of patients (Figure 6b). Regarding the relationship between TERT expression and *ATRX* mutation, we inferred that patients with ALT, which can occur due to loss of *ATRX*, have poorer prognosis than patients who have higher TERT expression.

EGFR signaling induces proliferation, which is one of the common events in various types of cancer [47]. Interestingly, the occurrence of *EGFR* mutation increased with aging and was independent of its occurrence with *IDH1*, *TP53*, and *ATRX* mutations (Figure 1a, 4a, and 7c). Unlike in patients with GBM, *EGFR* mutation occurred frequently in older patients with LGG. Patients with LGG harboring *EGFR* mutation showed poor prognosis for both grade 2 and 3; however, *EGFR* mutation in GBM did not affect prognosis (Figure 7a). After conducting multi-label IG and pathway enrichment analysis, most of the related pathways were found to be involved in the regulation of the cell cycle and cell signaling. Cell-cycle related pathways were downregulated and transcriptional regulation by VENTX was upregulated in grade 3 glioma and GBM. Detoxification of reactive oxygen species and interleukin-12 (IL-12) signaling, which exert an antitumor effect on tumors, including glioma and glioblastoma, were downregulated in grade 3 glioma and GBM [48-51].

In conclusion, mutations of *IDH1*, *TP53*, and *ATRX* occur in early-onset glioma, whereas *EGFR* mutation is associated with late-onset glioma. Interestingly, these mutations are associated with the WHO central nervous system tumor classifications. We believe that our results regarding mutations in *IDH1*, *TP53*, *ATRX* and *EGFR* can be applied to classify glioma according to age and precisely predict the prognosis of glioma. Furthermore, the results of transcriptomic analysis can suggest molecular theraputic targets of age dependent glioma.

4. Materials and Methods

4.1. Description of TCGA Data and Entire Analysis Process

Transcriptome sequencing and clinical data of GBM and low-grade glioma were downloaded from the UCSC Xena database. The tumor statuses were LGG (n = 508) and GBMLGG (n = 657), and all the samples of the GBMLGG dataset were primary tumors (n = 657). All samples used in this study have clinical data, survival data, non-silent somatic mutation data, and transcriptomic data. The description of entire analysis process are visualized in flow chart (Figure 8).

Preprints (www.preprints.org) | NOT PEER-REVIEWED | Posted: 23 February 2021 doi:10.20944/preprints202102.0501.v1

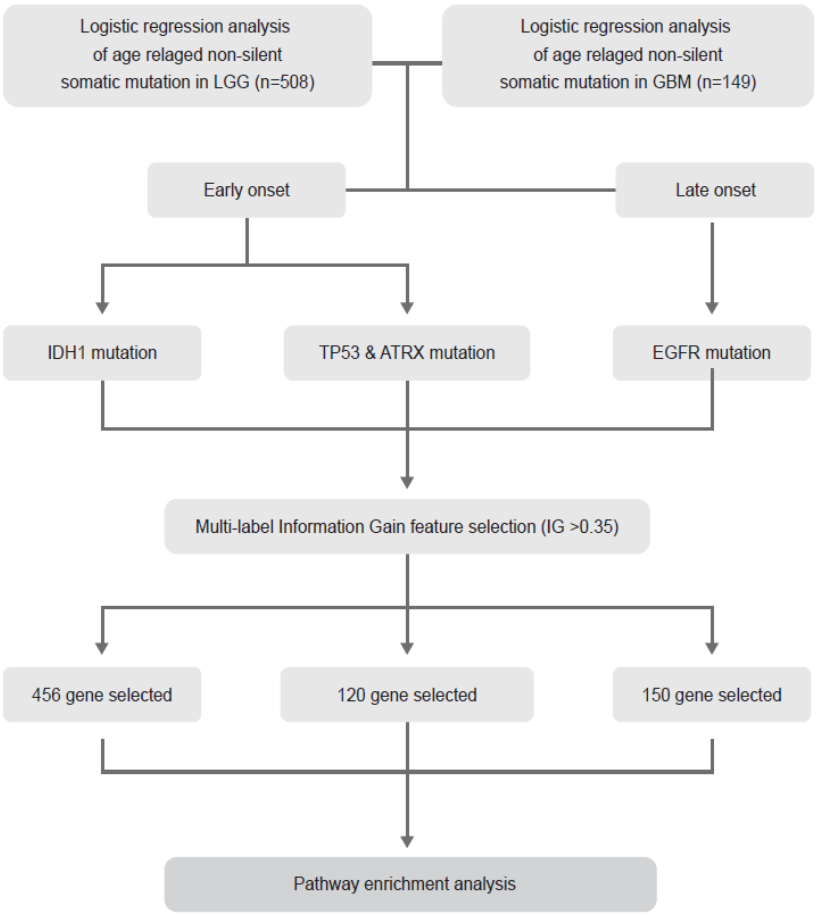

Figure 8. The flow chart of entire process of analysis.

4.2. Extraction of Candidate Somatic Mutations Related to Age

Candidate somatic mutations related to ages were selected based on a somatic mutation rate of at least 5% from somatic mutation data from multi-center mutation calling (MC3). Somatic mutation rate is calculated by individual who has mutation/all individuals. Logistic regression analysis was performed to identify somatic mutations related to age. Bonferroni correction was conducted to correct the p-value of logistic regression. Logistic regression analysis was conducted by binomial and corrected p-value which is 0.05 and 95 percent confidence intervals. The somatic mutation rate and results of logistic regression were visualized using forest plot v 1.10 (http://gforge.se/packages/)

4.3. Comparing Age with Mutation Status and Grade

The relationship between non-silent somatic mutations selected by logistic regression analysis and onset age are validated by comparing age at initial pathologic diagnosis with each mutations and grade. These results are visualized by ggpubr (https://rpkgs.datanovia.com/ggpubr/reference/ggboxplot.html).

4.4. Survival Analysis

Pairwise log-rank tests with Benjamini-Hochberg corrections were performed to compare prognoses between the groups, which were divided via agglomerative clustering with whole genes; Kaplan-Meier plots were generated in all survival analyses. Survival analysis was conducted using survival (https://CRAN.R-project.org/package=survival), and the survival plot was visualized using survminer (http://www.sthda.com/english/rpkgs/survminer/), both of which are R packages.

 doi:10.20944/preprints202102.0501.v1

4.5. Multi-label IG based feature selection

Mutil-labels, based on the histological grade and presence of somatic mutations in specific genes, were allotted to each individual. IG using multi-label individual and gene-level expression data was performed using FSlector v 0.31 [52, 53]. IG more than 0.35 was used as the feature selection threshold for the grade-mutation statuses of *IDH1*, *ATRX*, *TP53*, and *EGFR*.

4.6. Hierarchical Clustering and Heatmap with Annotations of Information

Hierarchical clustering of patients was performed by the gene expression levels of the gene set with an IG over 0.35. Visualization of hierarchical clustering data was performed using a Complex heatmap with annotation, which has information regarding tumor grade and genotype (mutant or wild-type) [54].

4.7. Pathway Enrichment Analysis

Reactome pathway enrichment analysis was performed using the ClueGo software, and significant pathways with Benjamini-Hochberg correction < 0.05 were extracted in Cytoscape [55]. p-values of the enriched pathways are presented as -log10 (p-value).

Supplementary Materials: The following are available online at www.mdpi.com/xxx/s1.

Author Contributions: Y.J. Park, J.M. Park and J.J. Lim contributed to the study conceptualization, study analysis, manuscript writing with the feedback from K.S. Sung. Y.J. Park, J.M. Park, J.W. Ahn, S.W. Kim and J.M. Shim processed genome data curation for public data base and performed bioinformatic analyses. S.J. Kang assisted in visualization and genome data curation. S.J. Hwang, K.S. Sung and J.J. Lim contributed to clinical data interpretation. J.J. Lim and K.S. Sung supervised the entire project and approved the final manuscript submission.

Funding: Basic Science Research Program through the National Research Foundation of Korea (NRF), funded by the Korea Government (MSIT) (Grant No. 2018R1C1B5086460).

Acknowledgments: The authors thank the National Research Foundation of Korea (NRF).

Conflicts of Interest: The authors declare no conflict of interest.

Data Availability Statement

Abbreviations

ALT	Alternative lengthening of telomere
APC/C	Anaphase-promoting complex/cyclosome
GBM	Glioblastoma multiforme
IG	Information gain
LGG	Lower grade glioma
OS	Overall survival
PFI	Progression free interval

References

1 Goodenberger, M.L.; Jenkins, R.B. Genetics of adult glioma. *Cancer Gen*. **2012**, *205*, 613–621.
2 Friedman, H.S.; Kerby, T.; Calvert, H. Temozolomide and treatment of malignant glioma. *Clin. Cancer Res*. **2000**, *6*, 2585–2597.
3 Ceccarelli, M.; Barthel, F.P.; Malta, T.M.; Sabedot, T.S.; Salama, S.R.; Murray, B.A.; Morozova, O.; Newton, Y.; Radenbaugh, A.; Pagnotta, S.M.; et al. Molecular profiling reveals biologically discrete subsets and pathways of progression in diffuse glioma. *Cell* **2016**, *164*, 550–563.
4 Clarke J, Butowski N, Chang S. Recent advances in therapy for glioblastoma. Archives of neurology. 2010;67(3):279-83.
5 White, M.C.; Holman, D.M.; Boehm, J.E.; Peipins, L.A.; Grossman, M.; Henley. S.J. Age and cancer risk: a potentially modifiable relationship. *Am. J. Prev. Med*. **2014**, *46*, :S7–S15.
6 Vijg, J. Somatic mutations, genome mosaicism, cancer and aging. *Cur. Opin. Gen. Dev.* **2014**, *26*, 141–149.
7 Martincorena, I.; Campbell, P.J. Somatic mutation in cancer and normal cells. *Science* **2015**, *349*, 1483–1489.
8 Yates, L.R.; Campbell, P.J. Evolution of the cancer genome. *Nat. Rev. Genet*. **2012**, *13*, 795–806.

9 Greenman, C.; Stephens, P.; Smith, R.; Dalgliesh, G.L.; Hunter, C.; Bignell, G.; Davies, H.; Teague, J.; Butler, A.; Stevens, C.; et al. Patterns of somatic mutation in human cancer genomes. *Nature* **2007**, *446*, 153–158.

10 Grist, S.; McCarron, M.; Kutlaca, A.; Turner, D.; Morley, A. In vivo human somatic mutation: frequency and spectrum with age. *Mutat. Res.* **1992**, *266*, 189–196.

11 Yan, H.; Parsons, D.W.; Jin, G.; McLendon, R.; Rasheed, B.A.; Yuan, W.; Kos, I.; Batinic-Haberle, I.; Jones, S.; Riggins, G.J.; et al. *IDH1* and IDH2 mutations in gliomas. *New Engl. J. Med*. **2009**, *360*, 765–773.

12 Zhong, Z.; Wang, Z.; Wang, Y.; You, G.; Jiang, T. *IDH1*/2 mutation is associated with seizure as an initial symptom in low-grade glioma: a report of 311 Chinese adult glioma patients. *Epilepsy Res*. **2015**, *109*, 100–105.

13 Wang, T-X.; Liang, J-Y.; Zhang, C.; Xiong, Y.; Guan, K-L.; Yuan, H-X. The oncometabolite 2-hydroxyglutarate produced by mutant *IDH1* sensitizes cells to ferroptosis. *Cell Death Dis*. **2019**, *10*, 1–12.

14 Modrek, A.S.; Golub, D.; Khan, T.; Bready, D.; Prado, J.; Bowman, C.; Deng, J.; Zhang, G.; Rocha, P.P.; Raviram, R.; et al. Low-grade astrocytoma mutations in *IDH1*, P53, and *ATRX* cooperate to block differentiation of human neural stem cells via repression of SOX2. *Cell Rep*. **2017**, *21*, 1267–1280.

15 Mu, L.; Long, Y.; Yang, C.; Jin, L.; Tao, H.; Ge, H.; Chang, Y.E.; Karachi, A.; Kubilis, P.S.; De Leon, G.; et al. The *IDH1* mutation-induced oncometabolite, 2-hydroxyglutarate, may affect DNA methylation and expression of PD-L1 in gliomas. *Front. Mol. Neurosci*. **2018**, *11*, 82.

16 Nicolas-Boluda, A.; Vaquero, J.; Barrin, S.; Kantari-Mimoun, C.; Ponzo, M.; Renault, G.; Deptula, P.; Pogoda, K.; Bucki, R.; Cascone, I.; et al. Tumor stiffening reversion through collagen crosslinking inhibition improves T cell migration and anti-PD-1 treatment. *BioRxiv*. **2020**.

17 Kwaan, H.C.; Lindholm, P.F. editors. *Fibrin and fibrinolysis in cancer. Seminars in thrombosis and hemostasis*, Thieme Medical Publishers, 2019.

18 Melrose, J. Keratan sulfate (KS)-proteoglycans and neuronal regulation in health and disease: the importance of KS-glycodynamics and interactive capability with neuroregulatory ligands. *J. Neurochem*. **2019**, *149*, 170–194.

19 O'Regan, L.; Blot, J.; Fry, A.M. Mitotic regulation by NIMA-related kinases. *Cell Div*. **2007**, *2*, 25.

20 Osmani, S.A.; Pu, R.T.; Morris, N.R. Mitotic induction and maintenance by overexpression of a G2-specific gene that encodes a potential protein kinase. *Cell* **1988**, *53*, 237–244.

21 Machida, Y.J.; Dutta, A. The APC/C inhibitor, Emi1, is essential for prevention of rereplication. *Genes Dev*. **2007**, *21*, 184–194.

22 Qiao, R.; Weissmann, F.; Yamaguchi, M.; Brown, N.G.; VanderLinden, R.; Imre, R.; Jarvis, M.A.; Brunner, M.R.; Davidson, I.F.; Litos, G.; et al. Mechanism of APC/CCDC20 activation by mitotic phosphorylation. *Proc. Natl. Acad. Sci*. **2016**, *113*, E2570–E2578.

23 Boekhout, M.; Wolthuis, R. Nek2A destruction marks APC/C activation at the prophase-to-prometaphase transition by spindle-checkpoint-restricted Cdc20. *J. Cell Sci*. **2015**, *128*, 1639–1653.

24 Huang, J.S.; Guh, J.Y.; Chen, H.C.; Hung, W.C.; Lai, Y.H.; Chuang, L.Y. Role of receptor for advanced glycation end-product (RAGE) and the JAK/STAT-signaling pathway in AGE-induced collagen production in NRK-49F cells. *J. Cell. Biochem*. **2001**, *81*, 102–113.

25 Cattaneo, F.; Guerra, G.; Ammendola, R. Expression and signaling of formyl-peptide receptors in the brain. *Neurochem. Res*. **2010**, *35*, 2018–2026.

26 Yan, K.; Wu, Q.; Yan, D.H.; Lee, C.H.; Rahim, N.; Tritschler, I.; DeVecchio, J.; Kalady, M.F.; Hjelmeland, A.B.; Rich, J.N. Glioma cancer stem cells secrete Gremlin1 to promote their maintenance within the tumor hierarchy. *Genes Dev*. **2014**, *28*, 1085–1100.

27 Oeck, S.; Al-Refae, K.; Riffkin, H.; Wiel, G.; Handrick, R.; Klein, D.; Iliakis, G.; Jendrossek, V. Activating Akt1 mutations alter DNA double strand break repair and radiosensitivity. *Sci. Rep*. **2017**, *7*, 42700.

28 Jiramongkol, Y.; Lam, EW-F. FOXO transcription factor family in cancer and metastasis. *Cancer Metastasis Rev*. **2020**, 1–29.

29 Cheng, F.; Guo, D. MET in glioma: signaling pathways and targeted therapies. *J. Exp. Clin. Cancer Res*. **2019**, *38*, 270.

30 Jäättelä, M. Multiple cell death pathways as regulators of tumour initiation and progression. *Oncogene* **2004**, *23*, 2746–2756.

31 Olivier, M.; Hollstein, M.; Hainaut, P. *TP53* mutations in human cancers: origins, consequences, and clinical use. *Cold Spring Harb. Perspect. Biol*. **2010**, *2*, a001008.

32 Rasheed, B.A.; McLendon, R.E.; Herndon, J.E.; Friedman, H.S.; Friedman, A.H.; Bigner, D.D.; Bigner, S.H. Alterations of the *TP53* gene in human gliomas. *Cancer Res*. **1994**, *54*, 1324–1330.

33 Amorim, J.P.; Santos, G.; Vinagre, J.; Soares, P. The role of *ATRX* in the alternative lengthening of telomeres (ALT) phenotype. *Genes* **2016**, *7*, 66.

34 Haase, S.; Garcia-Fabiani, M.B.; Carney, S.; Altshuler, D.; Núñez, F.J.; Méndez, F.M.; Nunez, F.; Mendez, F.M.; Lowenstein, P.R.; Castro, M.G. Mutant *ATRX*: uncovering a new therapeutic target for glioma. *Expert Opin. Ther. Targets*. **2018**, *22*, 599–613.

35 Elsässer, S.J.; Allis, C.D.; Lewis, P.W. New epigenetic drivers of cancers. *Science* **2011**, *331*, 1145–1146.

 doi:10.20944/preprints202102.0501.v1

36 Liu, J.; Zhang, X.; Yan, X.; Sun, M.; Fan, Y.; Huang, Y. Significance of *TERT* and *ATRX* mutations in glioma. *Oncol. Lett*. **2019**, *17*, 95–102.

37 Schwartzentruber, J.; Korshunov, A.; Liu, X-Y.; Jones, D.T.; Pfaff, E.; Jacob, K.; Sturm, D.; Fontebasso, A.M.; Khuong Quang, D-A.; Tonjes, M.; et al. Driver mutations in histone H3. 3 and chromatin remodelling genes in paediatric glioblastoma. *Nature* **2012**, *482*, 226–231.

38 Yuan, X.; Larsson, C.; Xu, D. Mechanisms underlying the activation of *TERT* transcription and telomerase activity in human cancer: old actors and new players. *Oncogene* **2019**, *38*, 6172–6183.

39 Hanahan, D.; Weinberg, R.A. Hallmarks of cancer: the next generation. *Cell* **2011**, *144*, 646–674.

40 Liu, T.; Yuan, X.; Xu, D. Cancer-specific telomerase reverse transcriptase (*TERT*) promoter mutations: biological and clinical implications. *Genes* **2016**, *7*, 38.

41 Barthel, F.P.; Wei, W.; Tang, M.; Martinez-Ledesma, E.; Hu, X.; Amin, S.B.; Akdemir, K.C.; Seth, S.; Song, X.; Wang, Q.; et al. Systematic analysis of telomere length and somatic alterations in 31 cancer types. *Nat. Genet*. **2017**, *49*, 349–357.

42 Oppel, F.; Tao, T.; Shi, H.; Ross, K.N.; Zimmerman, M.W.; He, S.; Tong, G.; Aster, J.C.; Look, A.T. Loss of *ATRX* cooperates with p53-deficiency to promote the development of sarcomas and other malignancies. *PLoS Genet*. **2019**, *15*, e1008039.

43 Idilli, A.I.; Cusanelli, E.; Pagani, F.; Berardinelli, F.; Bernabé, M.; Cayuela, M.L.; Poliani, P.L.; Mione, M.C. Expression of *TERT* prevents ALT in zebrafish brain tumors. *Front. Cell Dev. Biol*. **2020**, *8*, 65.

44 Lafferty-Whyte, K.; Cairney, C.J.; Will, M.B.; Serakinci, N.; Daidone, M-G.; Zaffaroni, N.; Bilsland, A.; Keith, W.N. A gene expression signature classifying telomerase and ALT immortalization reveals an h*TERT* regulatory network and suggests a mesenchymal stem cell origin for ALT. *Oncogene* **2009**, *28*, 3765–3774.

45 Deeg, K.I.; Chung, I.; Poos, A.M.; Braun, D.M.; Korshunov, A.; Oswald, M.; Kepper, N.; Bender, S.; Castel, D.; Lichter, P.; et al. Dissecting telomere maintenance mechanisms in pediatric glioblastoma. *BioRxiv*. **2017**, 129106.

46 Chen, R-J.; Wu, P-H.; Ho, C-T.; Way, T-D.; Pan, M-H.; Chen, H-M.; Ho, Y-S.; Wang, Y-J. P53-dependent downregulation of h*TERT* protein expression and telomerase activity induces senescence in lung cancer cells as a result of pterostilbene treatment. *Cell Death Dis*. **2017**, *8*, e2985.

47 Hatanpaa, K.J.; Burma, S.; Zhao, D.; Habib, A.A. Epidermal growth factor receptor in glioma: signal transduction, neuropathology, imaging, and radioresistance. *Neoplasia* **2010**, *12*, 675–684.

48 Liou, G-Y.; Storz, P. Reactive oxygen species in cancer. *Free Radic. Res*. **2010**, *44*, 479–496.

49 Singer, E.; Judkins, J.; Salomonis, N.; Matlaf, L.; Soteropoulos, P.; McAllister, S.; Soroceanu, L. Reactive oxygen species-mediated therapeutic response and resistance in glioblastoma. *Cell Death Dis*. **2015**, *6*, e1601.

50 Kim, S.H.; Kwon, C.H.; Nakano, I. Detoxification of oxidative stress in glioma stem cells: mechanism, clinical relevance, and therapeutic development. *J. Neurosci. Res*. **2014**, *92*, 1419–1424.

51 Weiss, T.; Puca, E.; Silginer, M.; Hemmerle, T.; Pazahr, S.; Bink, A.; Weller, M.; Neri, D.; Roth, P. Immunocytokines are a promising immunotherapeutic approach against glioblastoma. *Sci. Transl. Med*. **2020**, *12*.

52 Cheng, T.; Wang, Y.; Bryant, S.H. FSelector: a Ruby gem for feature selection. *Bioinformatics* **2012**, *28*, 2851–2852.

53 Romanski, P.; Kotthoff, L.; Kotthoff, M.L. Package 'FSelector'. *Repository CRAN*. **2018**, 1–18.

54 Gu, Z.; Eils, R.; Schlesner, M. Complex heatmaps reveal patterns and correlations in multidimensional genomic data. *Bioinformatics* **2016**, *32*, 2847–2849.

55 Bindea, G.; Mlecnik, B.; Hackl, H.; Charoentong, P.; Tosolini, M.; Kirilovsky, A.; et al. ClueGO: a Cytoscape plug-in to decipher functionally grouped gene ontology and pathway annotation networks. *Bioinformatics* **2009**, *25*, 1091–1093.